

1 *Conference Proceedings Paper*

## 2 **Analysis of dry and wet episodes in eastern South** 3 **America during 1980-2018 using SPEI**

4 **Anita Drumond<sup>1\*</sup>, Milica Stojanovic<sup>2</sup>, Raquel Nieto<sup>3</sup>, Luis Gimeno<sup>3</sup>, Margarida L.R. Liberato<sup>2,4</sup>,**  
5 **Tercio Ambrizzi<sup>5</sup>, Theotonio Pauliquevis<sup>1</sup> and Marina de Oliveira<sup>1</sup>**

6 1 Instituto de Ciências Ambientais, Químicas e Farmacêuticas, Universidade Federal de São Paulo,  
7 Diadema 09913-030, Brazil; theotonio.pauliquevis@unifesp.br, oliveira.marina@unifesp.br

8 2 Instituto Dom Luiz, Faculdade de Ciências da Universidade de Lisboa, 1749-016, Campo Grande,  
9 Portugal; mstojanovic@fc.ul.pt, mlr@utad.pt

10 3 Environmental Physics Laboratory (EPhysLab), CIM-Uvigo, Universidade de Vigo, 32004, Ourense,  
11 Spain; rnieto@uvigo.es, l.gimeno@uvigo.es

12 4 Escola de Ciências e Tecnologia, Universidade de Trás-os-Montes e Alto Douro, 5001-801 Vila Real,  
13 Portugal

14 5 Departamento de Ciências Atmosféricas, IAG, Universidade de São Paulo, São Paulo, 05508-090, Brazil;  
15 tercio.ambrizzi@iag.usp.br

16 \* Correspondence: anita.drumond@unifesp.br

17 Received: date; Accepted: date; Published: date

18 **Abstract:** A large part of the population and the economic activities of South America are located in  
19 eastern continent (ESA), where extreme climate dry and wet episodes are a recurrent phenomenon.  
20 Besides other oceanic and terrestrial sources, the precipitation over ESA may be modulated by air  
21 masses from the subtropical South Atlantic along the year. This study analyzes the extreme climate  
22 conditions at domain-scale occurring over ESA in the last four decades through the multi-scalar  
23 Standardized Precipitation-Evapotranspiration Index (SPEI). The study area was defined according  
24 to the results of a Lagrangian approach developed for moisture analysis. It consists in the major  
25 continental sink of the moisture transported from the Subtropical South Atlantic Ocean towards  
26 South America, comprising the Amazonia, almost all the Brazilian territory, and La Plata regions.  
27 The SPEI for 1-, 3-, 6-, and 12-months of accumulation was calculated for the period 1980-2018 using  
28 monthly CRU (TS4.03) precipitation and potential evapotranspiration time series averaged on the  
29 study area. The wet and dry climate conditions were identified and classified through the SPEI  
30 values (mild, moderate, severe, and extreme). The results indicate the predominance of dry  
31 conditions in the decade of 2010, while wet periods prevailed in the 1990s and 2000s.

32 **Keywords:** SPEI; eastern South America; extreme climate conditions; drought; wet episodes  
33

---

### 34 1. Introduction

35 It is known that climate change may affect the frequency and intensity of extreme climate events  
36 [1]. In the last decades, South America has suffered from the alternation of extremely wet and dry  
37 climate conditions [2-5]. Currently, the dry conditions observed over the Amazon rainforest and the  
38 Pantanal wetlands during 2020 are an example of how drought events could enhance the propagation  
39 of fires, with enormous socio economic and environmental damages [e.g., 6]. In the last decade, the  
40 2014 drought over Southeastern Brazil affected the water supply in the Metropolitan Area of Sao  
41 Paulo (MASP), one of the most populous areas in South America [3]. On the other hand, the observed  
42 positive trend in the frequency and intensity of extreme rainfall events in MASP, particularly during  
43 the austral Summer, triggers flash floods and landslides over the area [7,8]. The increasing number

44 of consecutive dry days also observed in MASP [8] indicates that intense precipitation is concentrated  
45 in fewer days, separated by longer dry spells.

46 Focusing on how the atmospheric circulation may contribute to these climate changes in MASP,  
47 Marengo et al. [8] verified that during the last six decades the South Atlantic Subtropical High (SASH)  
48 has intensified and slightly moved southwestward of its normal position, probably affecting the  
49 transport of humidity towards South America and the precipitation associated.

50 The importance of the South Atlantic as one of the major oceanic sources of moisture in the globe  
51 and its contribution to the precipitation over different regions located in eastern South America (ESA)  
52 has already been reported in previous works, such as the ones based on the Lagrangian approach  
53 developed by Stohl and James [9,10] to analyze moisture transport [e.g 5; 11-17]. These works pointed  
54 out the joint role of the moisture transport predominantly by air masses from the Tropical North  
55 Atlantic and the South Atlantic to the precipitation over ESA, besides the terrestrial sources.  
56 However, a systematic definition of the region which consists as a climatological sink of the moisture  
57 transported by air masses from the South Atlantic, and an identification of the associated extreme  
58 climate periods at domain-scale has not been conducted yet.

59 Therefore, this work aims to identify the extreme wet and dry periods at domain-scale over ESA  
60 during 1980-2018 through the multi-scalar Standardized Precipitation-Evapotranspiration Index  
61 (SPEI) [18]. The SPEI includes precipitation (PRE) and potential evapotranspiration (PET) in  
62 calculation of anomalies in climatic water balance. It was calculated at 1-, 3-, 6-, and 12-months  
63 allowing the identification of extreme conditions at different accumulation periods, which may affect  
64 different components of the hydrological cycle.  
65

## 66 2. Data and Methodology

### 67 2.1. Data

68 The analysis covers the period from 1980 to 2018. ERA-Interim global reanalysis dataset from  
69 the European Centre for Medium-Range Weather Forecasts (ECMWF) [19], with a horizontal  
70 resolution of 1° on 61 vertical levels from the surface to 0.1 hPa, is used both in the identification of  
71 the South Atlantic moisture source region and as input for FLEXPART model. According to Gimeno  
72 et al. [14], ERA-Interim reanalysis data are appropriate to feed the model because of the high-quality  
73 data for wind and humidity required by FLEXPART, besides the reproduction of the hydrological  
74 cycle in a satisfactory way. The dataset are available at  
75 <https://www.ecmwf.int/en/forecasts/datasets/archive-datasets/reanalysis-datasets/era-interim>.

76 The SPEI was computed using datasets of PRE and PET from the Climate Research Unit (CRU)  
77 Time-Series (TS) Version 4.03 [20] at a spatial resolution of 0.5°. Data are available at  
78 <https://catalogue.ceda.ac.uk/uuid/10d3e3640f004c578403419aac167d82>.

### 79 2.2. Lagrangian approach for the analysis of moisture transport

80 The South Atlantic moisture source region (SAT) was firstly defined by Gimeno et al. [13,14],  
81 based on the maxima of the annual climatological vertically integrated moisture flux (VIMF)  
82 divergence (values higher than 750 mm/year, which corresponds to approximately the 60<sup>th</sup> percentile  
83 of the positives values from the respective global climatology on the annual scale).

84 The same methodology of Gimeno et al. [13-14] for the identification of the SAT moisture sinks  
85 at seasonal scale was applied here, but now the sink was defined on annual basis. More details of the  
86 Lagrangian approach applied here for the identification of major moisture sinks for oceanic sources  
87 may be found in [13,14]. In comparison with the Eulerian approaches [e.g., 21], the Lagrangian  
88 methodology enables the tracking of air parcels, allowing the establishment of moisture source–

receptor relationships in a more realistic way [22]. The Lagrangian approach applied here was developed by Stohl and James [9,10] and it is based on the FLEXPART (FLEXiblePARTicle dispersion model, [9]). In the FLEXPART simulation, the global atmosphere was divided homogenously into nearly 2.0 million particles with constant mass transported using 3D wind fields from the global reanalysis data ERA-Interim. The changes in specific humidity ( $q$ ) of each particle along its path were computed every 6h, and they can be expressed as:  $e-p=m(dq/dt)$  where  $m$  is the mass of the particle and  $e-p$  represents the freshwater flux associated with each particle (evaporation  $e$  minus precipitation  $p$ ). The total  $(E-P)$  represents the surface freshwater flux associated with the tracked particles per unit area and was obtained by adding  $(e-p)$  for all the particles residing in the atmospheric column over a given area.

In this study, the trajectories were tracked forward in time to identify the sinks of the moisture (areas where the particles lost moisture  $E - P < 0$ ) transported by particles leaving the SAT moisture source and tracked for a period of 10 days (i.e., the average residence time of water vapor in the atmosphere [23]). The orange area in Figure 1 (left) delimits the major moisture sink area in South America selected using the 90th percentile of the negative part of  $(E - P)$  (i.e.,  $-0.1 \text{ mm day}^{-1}$ ) obtained from the respective global climatology (from 1980 to 2018) on the annual scale.

### 2.3. Extreme wet and dry climate periods identification and analysis

Following the method applied by Drumond et al. [5] and Stojanovic et al. [24], 1-, 3-, 6-, and 12-months SPEI time scales for 1980-2018 are calculated through time series of monthly PRE and PET with the purpose to identify the domain-scale extreme wet and dry climate periods occurred over the ESA region.

SPEI was first proposed by Vicente-Serrano et al. [18] as an improved drought index that is particularly suitable for studying the effect of global warming on drought severity [25]. The SPEI follows the same conceptual approach as the Standardized Precipitation Index (SPI) [26-28], but it is based on a monthly climatic water balance (precipitation minus evapotranspiration) rather than on precipitation solely. The climatic water balance is calculated at various time scales (i.e. accumulation periods), and the resulting values are fit to a log-logistic probability distribution to transform the original values to standardized units that are comparable in space and time and at different SPEI time scales. Details of the SPEI calculation can be found in [18,29,30].

The criteria proposed by McKee et al. [26] based on the SPI value is applied in the present work to characterize the domain-scale wet and dry periods according to the SPEI values (Table 1).

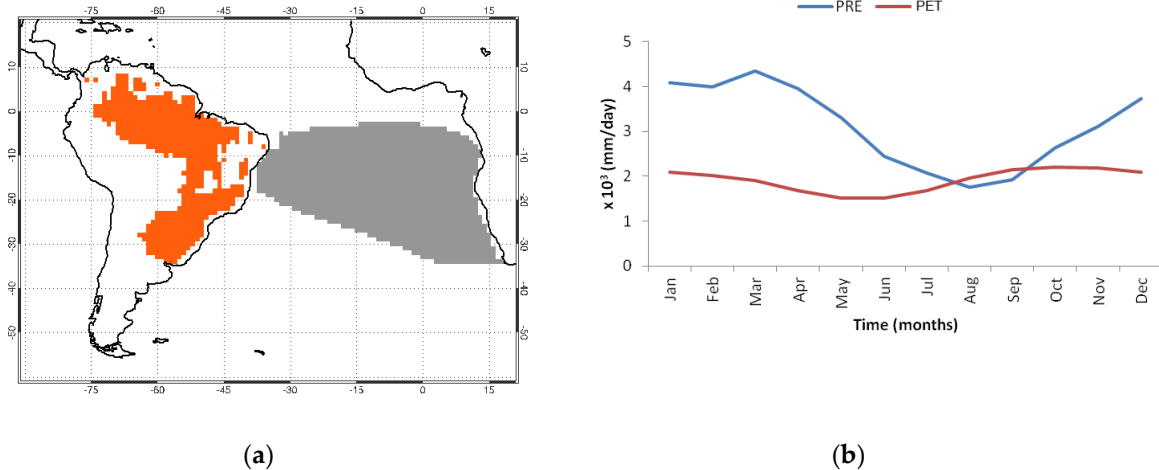
**Table 1.** Classification of SPEI values according to their magnitude. Adapted from [26]

SPEI values	Category
2.0 and more	Extremely wet
1.5 to 1.99	Severely wet
1.0 to 1.49	Moderately wet
0.0 to 0.99	Mild wet
-0.99 to 0.0	Mild dry
-1.0 to -1.49	Moderately dry
-1.5 to -1.99	Severely dry
-2.0 and less	Extremely dry

## 3. Results and Discussion

Figure 1a shows a schematic representation of the South Atlantic moisture source (grey) and its major sink over South America (ESA, orange) identified according to Gimeno et al.[13,14]. The source is placed over the South Atlantic Subtropical High region, the main feature of the atmospheric circulation over the South Atlantic Ocean which affects the South American and African weather and climate [31]. In the South American continent, the Lagrangian approach results show that during the

129 year the moisture transported by air masses from the South Atlantic precipitates mainly over the  
130 Amazon, Central Brazil and southeastern continental regions, configuring an area affected by the  
131 South American monsoon system [32]. In terms of the climatological annual cycle of the freshwater  
132 flux (PRE-PET) over the ESA (Figure 1b), PRE prevailed over PET during the year, except from  
133 August to September. Climatological PRE presents a well-defined annual cycle over the ESA,  
134 characterized by rainier Summer months and a drier Winter season. Climatological PET over the ESA  
135 presents a minimum in the late Autumn season.  
136

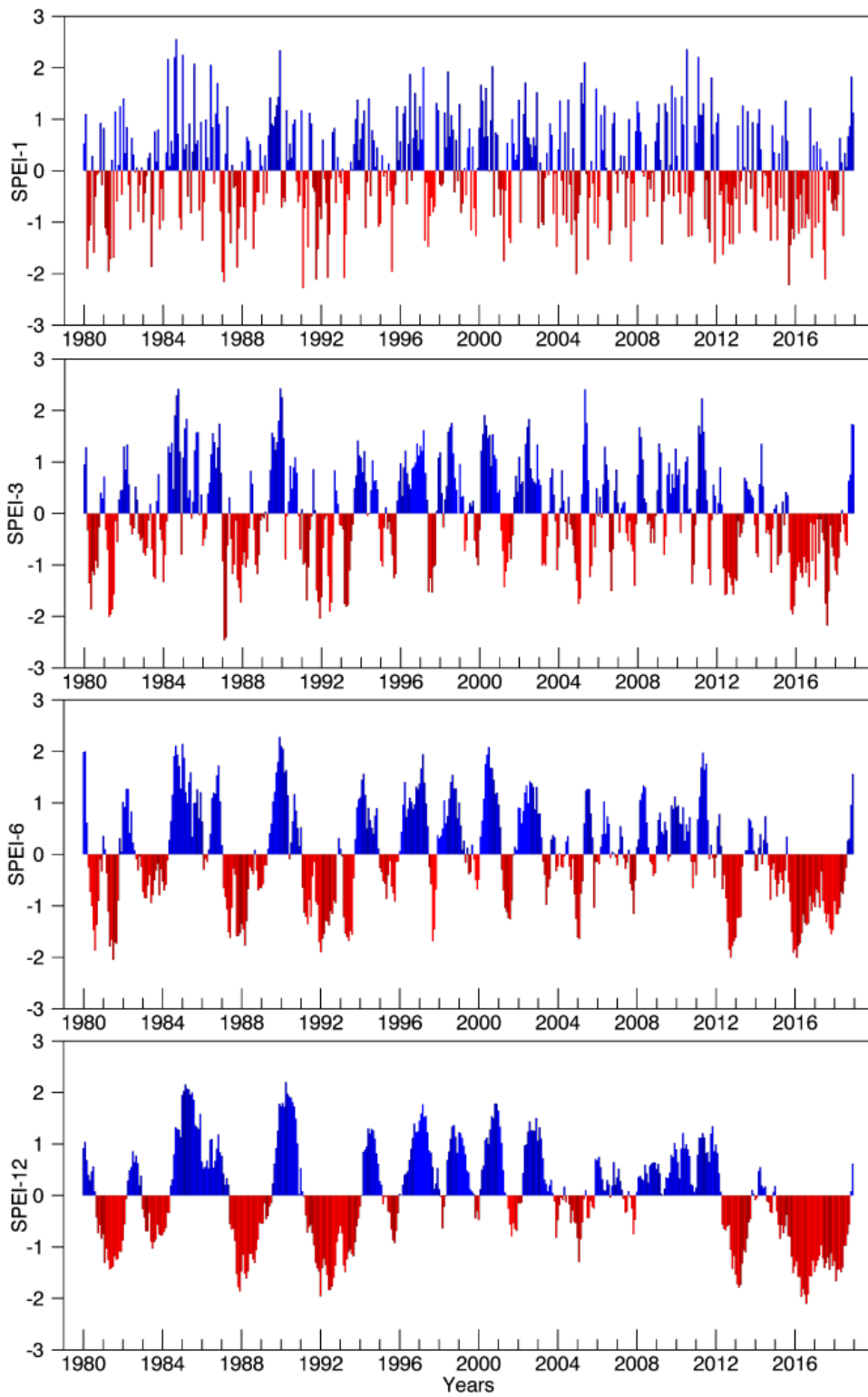


137 **Figure 1.** (a) Schematic representation of the South Atlantic source (grey) identified using the  
138 maximum vertically integrated moisture flux divergence according to Gimeno et al. [13,14] and its  
139 respective moisture sink over eastern South America (ESA, orange) defined using a forward-in-time  
140 experiment; (b) The annual climatological precipitation cycle (PRE, blue line) and potential  
141 evapotranspiration (PET, red line) integrated over the ESA for 1980–2018. Scale: mm/day. Data are  
142 from the CRU TS 4.03.  
143

144 Figure 2 shows the time series of the SPEI on the scale of 1-, 3-, 6-, and 12-months over ESA to  
145 illustrate the evolution of the index on different time scales (conditions accumulated over monthly,  
146 seasonal, semiannual, and annual periods, respectively). Positive values in blue indicate wet periods,  
147 and negative values in red show dry conditions. Looking at Figure 2, one can see the predominance  
148 of wet periods during mid-90s and the decade of 2000, and of dry conditions during the decade of  
149 2010.

150 Looking at how wet and dry conditions (and the magnitude associated) over ESA varied during  
151 the decades, Figure 3 shows the number of occurrence of SPEI-1, -3, -6, and -12 values at each one of  
152 the categories defined in Table 1 during the periods of 1980-89, 1990-99, 2000-09, and 2010-18. This  
153 figure confirms the predominance of wet conditions during the decade of 2000. On the other hand,  
154 Figure 3 confirms that the period 2010-2018 (even shorter in comparison with the remaining decades)  
155 concentrates the highest number of occurrences of dry SPEI values, particularly in the categories  
156 moderate and severe (at the scales -6 and -12). It deserves to mention that the extremely dry  
157 conditions were reached in the four accumulation scales during 2010-2018; moreover, the only  
158 extreme dry value at SPEI-12 was registered during this decade.

159 A joint analysis of dry and wet conditions at the different accumulation periods reveals that  
160 extreme wet conditions also occurred during the decade of 1980, although it was predominantly dry  
161 at seasonal, semiannual and annual accumulation scales. A similar pattern was verified for the  
162 predominant dry conditions (reaching the category extreme) during the 1990's at the SPEI-1 scale in  
163 contrast to the wet conditions prevailing at the remaining scales.  
164



165  
166  
167

**Figure 2.** Time series of SPEI-1, SPEI-3, SPEI-6, and SPEI-12 for the ESA during 1980–2018. Data are computed from CRU TS 4.03.

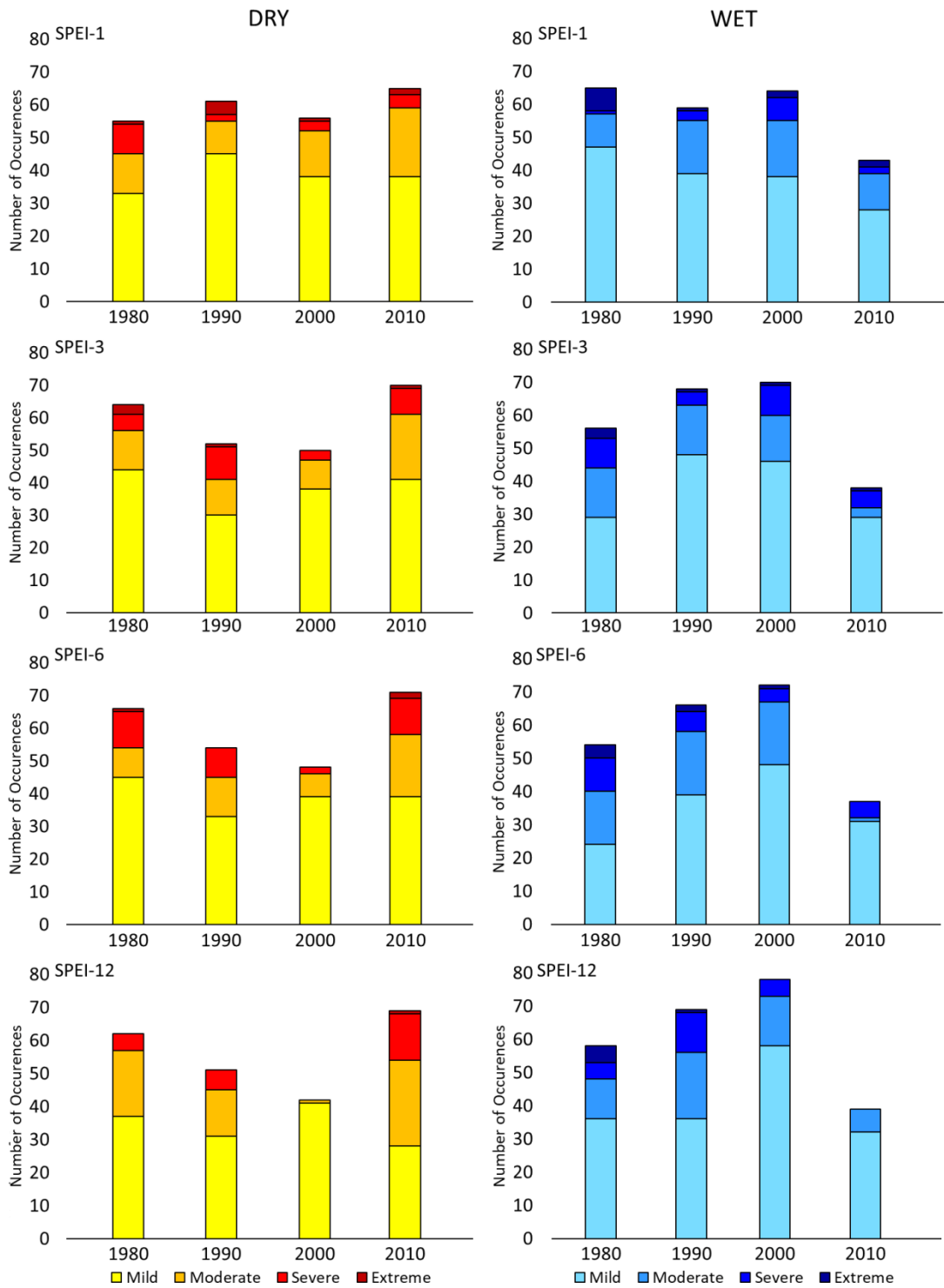


**Figure 3.** Number of occurrence of ESA SPEI-1, SPEI-3, SPEI-6, and SPEI-12 values at each one of the categories defined in Table 1 during the periods 1980-89, 1990-99, 2000-09, and 2010-18. Data are computed from CRU TS 4.03.

168  
 169  
 170  
 171  
 172  
 173

#### 174 4. Conclusions

175 In the present study, the dry and wet climate periods at domain-scale occurring over the eastern  
176 South American (ESA) region during 1980-2018 were identified and characterized through the multi-  
177 scalar Standardized Precipitation-Evapotranspiration Index (SPEI) at the SPEI-1, SPEI-3, SPEI-6, and  
178 SPEI-12 months accumulation periods. The spatial domain of ESA covers an area extending from the  
179 Amazon, crossing central Brazil, and reaching the southeastern continental areas, and it consists in  
180 the major continental sink of the moisture transported from the Subtropical South Atlantic Ocean  
181 towards South America according to a Lagrangian approach developed for moisture transport  
182 analysis. The wet and dry climate conditions over ESA were identified and classified through the  
183 SPEI values (classified as mild, moderate, severe, and extreme). The main conclusions are then  
184 summarized:

- 185 • The climatological annual cycle of the freshwater flux over ESA shows that precipitation  
186 prevailed over potential evapotranspiration during the year, except from August to  
187 September. ESA is characterized by rainier Summer months and a drier Winter season;
- 188 • Although the decade of 1980 presented the highest number of extremely wet values in the  
189 SPEI-1, -3, -6, and -12 time series, it was also characterized by the predominance of dry values  
190 in the SPEI-3, -6 and -12 scales. In other words, results indicate that extreme wet and dry  
191 conditions occurred during this period;
- 192 • There was predominance of wet conditions during the decades of 1990 and 2000, except for  
193 the SPEI-1. It is worth to note that the decade of 1990 presented the highest number of  
194 extremely dry values in the SPEI-1 time series;
- 195 • The period of 2010-2018 (even shorter in comparison with the remaining decades)  
196 concentrates the highest number of occurrences of dry SPEI values. Extremely dry conditions  
197 were reached in the four accumulation scales during 2010-2018, and the only extreme dry  
198 value at SPEI-12 was registered during this decade.

199  
200 **Author Contributions:** Conceptualization and design of the calculations, AD, LG, TA; calculations, AD, MS,  
201 MO; analysis, AD, MS, RN, LG, ML, TA, TP, MO; writing—original draft preparation, AD; writing—review and  
202 editing, AD, MS, RN, LG, ML, TA. All authors have read and agreed to the published version of the manuscript.

203 **Funding:** MS and ML acknowledge funding from Fundação para a Ciência e a Tecnologia and Portugal  
204 Horizon2020 through project “Weather Extremes in the Euro Atlantic Region: Assessment and Impacts – WEx-  
205 Atlantic” (PTDC/CTA-MET/29233/2017). RN and LG thank the partially support by Xunta de Galicia under  
206 Project ED431C 2017/64-GRC “Programa de Consolidación e Estructuración de Unidades de Investigación  
207 Competitivas (Grupos de Referencia Competitiva)”, co-funded by the European Regional Development Fund,  
208 European-Union (FEDER). TA was supported by the National Institute of Science and Technology for Climate  
209 Change Phase 2 under CNPq Grant 465501/2014-1, FAPESP Grants 2014/50848-9 and 2017/09659-6; and also  
210 partially funded by CNPq grants 304298/2014-0 and 420262/2018-0. MO acknowledges the support received by  
211 PIBIC-CNPq (139943/2020-0) and FAPESP (2020/09548-2).

212 **Conflicts of Interest:** The authors declare no conflict of interest. The funders had no role in the design of the  
213 study; in the collection, analyses, or interpretation of data; in the writing of the manuscript, or in the decision to  
214 publish the results.

#### 215 References

- 216 1. Intergovernmental Panel on Climate Change (IPCC). Climate Change 2014: Synthesis Report; Contribution  
217 of Working Groups I, II and III to the Fifth Assessment Report of the Intergovernmental Panel on Climate  
218 Change; Pachauri, R.K., Meyer, L.A., Eds.; IPCC: Geneva, Switzerland, 2014; 151p. Available online:  
219 [https://www.ipcc.ch/pdf/assessment-report/ar5/syr/SYR\\_AR5\\_FINAL\\_full\\_wcover.pdf](https://www.ipcc.ch/pdf/assessment-report/ar5/syr/SYR_AR5_FINAL_full_wcover.pdf)
- 220 2. Marengo, J.A.; Nobre, C.A.; Tomasella, J.; Cardoso, M.F.; Oyama, M.D. Hydro-climatic and ecological  
221 behaviour of the drought of Amazonia in 2005. *Philos. Trans. R. Soc. B.*, **2008**, 363, 1773–1778.  
222 <https://doi.org/10.1098/rstb.2007.0015>

- 223 3. Coelho, C.A.S.; de Oliveira, C.P.; Ambrizzi, T.; Reboita, M.S.; Carpenedo, C.B.; Campos, J.L.P.S.;  
224 Tomaziello, A.C.N.; Pampuch, L.A.; de Souza Custódio, M.; Dutra, L.M.M.; Da Rocha, R.P.; Rehbein, A.  
225 The 2014 southeast Brazil austral summer drought: regional scale mechanisms and teleconnections. *Clim.*  
226 *Dyn.*, **2016**, 46(11), 3737–3752. <https://doi.org/10.1007/s00382-015-2800-1>
- 227 4. Garreaud, R.D.; Alvarez-Garretón, C.; Barichivich, J.; Boisier, J.P.; Christie, D.; Galleguillos, M.; LeQuesne,  
228 C.; McPhee, J.; Zambrano-Bigiarini, M. The 2010–2015 megadrought in Central Chile: impacts on regional  
229 hydroclimate and vegetation. *Hydrol. Earth Syst. Sci.*, **2017**, 21, 6307–6327. [https://doi.org/10.5194/hess-21-](https://doi.org/10.5194/hess-21-6307-2017)  
230 [6307-2017](https://doi.org/10.5194/hess-21-6307-2017)
- 231 5. Drumond, A.; Stojanovic, M.; Nieto, R.; Vicente-Serrano, S.M.; Gimeno, L. Linking anomalous moisture  
232 transport and drought episodes in the IPCC reference regions. *Bull. Am. Meteorol. Soc.*, **2019**, 100, 1481–1498.  
233 <https://doi.org/10.1175/BAMS-D-18-0111.1>
- 234 6. Brazil Fires Burn World’s Largest Tropical Wetlands at ‘Unprecedented’ Scale. Available online:  
235 <https://www.nytimes.com/2020/09/04/world/americas/brazil-wetlands-fires-pantanal.html> (accessed on 03  
236 October 2020)
- 237 7. Marengo, J.A.; Lincoln, M.A.; Ambrizzi, T.; Young, A.; Barreto, N.J.C.; Ramos, A.M. Trends in extreme  
238 rainfall and hydrogeometeorological disasters in the Metropolitan Area of São Paulo: a review. *Ann. N. Y.*  
239 *Acad. Sci.*, **2020a**, 1472(1), 5–20. <https://doi.org/10.1111/nyas.14307>
- 240 8. Marengo, J.A.; Ambrizzi, T.; Lincoln, M.A.; Barreto, N.J.C.; Reboita, M.S.; Ramos, A.M. Changing Trends  
241 in Rainfall Extremes in the Metropolitan Area of São Paulo: Causes and Impacts. *Front. Clim.*, **2020b**, 2(3),  
242 1–13. <https://doi.org/10.3389/fclim.2020.00003>
- 243 9. Stohl, A.; James, P. A Lagrangian Analysis of the Atmospheric Branch of the Global Water Cycle. Part I:  
244 Method Description, Validation, and Demonstration for the August 2002 Flooding in Central Europe. *J.*  
245 *Hydrometeorol.*, **2004**, 5, 656–678. [https://doi.org/10.1175/1525-7541\(2004\)005<0656:ALAOTA>2.0.CO;2](https://doi.org/10.1175/1525-7541(2004)005<0656:ALAOTA>2.0.CO;2)
- 246 10. Stohl, A.; James, P. A Lagrangian analysis of the atmospheric branch of the global water cycle: Part II:  
247 Moisture Transports between Earth’s Ocean Basins and River Catchments. *J. Hydrometeorol.*, **2005**, 6, 961–  
248 984. <https://doi.org/10.1175/JHM470.1>
- 249 11. Drumond, A.; Nieto, R.; Gimeno, L.; Ambrizzi, T. A Lagrangian identification of major sources of moisture  
250 over Central Brazil and La Plata Basin. *J. Geophys. Res. Atmos.*, **2008**, 113, D14128,  
251 <https://doi.org/10.1029/2007JD009547>
- 252 12. Drumond, A.; Nieto, R.; Gimeno, L.; Trigo, R.M.; Ambrizzi, T.; De Souza, E. A Lagrangian Identification of  
253 the Main Sources of Moisture Affecting Northeastern Brazil during Its Pre-Rainy and Rainy Seasons. *PLoS*  
254 *ONE*, **2010**, 5 (6), e11205. <https://doi.org/10.1371/journal.pone.0011205>
- 255 13. Gimeno, L.; Drumond, A.; Nieto, R.; Trigo, R.M.; Stohl, A. On the origin of continental precipitation.  
256 *Geophys. Res. Lett.*, **2010**, 37(13), L13804. <https://doi.org/10.1029/2010GL043712>
- 257 14. Gimeno, L.; Nieto, R.; Drumond, A.; Castillo, R.; Trigo, R.M. Influence of the intensification of the major  
258 oceanic moisture sources on continental precipitation. *Geophys. Res. Lett.*, **2013**, 40, 1443–1450.  
259 <https://doi.org/10.1002/grl.50338>
- 260 15. Drumond, A.; Marengo, J.M.; Ambrizzi, T.; Nieto, R.; Moreira, L.; Gimeno, L. The role of Amazon Basin  
261 moisture on the atmospheric branch of the hydrological cycle: a Lagrangian analysis. *Hydrol. Earth Syst.*  
262 *Sci.*, 2014, 18, 2577–2598. <https://doi.org/10.5194/hess-18-2577-2014>
- 263 16. Pampuch, L.A.; Drumond, A.; Gimeno, L.; Ambrizzi, T. Anomalous patterns of SST and moisture sources  
264 in the South Atlantic Ocean associated with dry events in southeastern Brazil. *Int. J. Climatol.* **2016**, 36, 4913–  
265 4928. <https://doi.org/10.1002/joc.4679>
- 266 17. Sorí, R.; Marengo, J.M.; Nieto, R.; Drumond, A.; Gimeno, L. The Atmospheric Branch of the Hydrological  
267 Cycle over the Negro and Madeira River Basins in the Amazon Region. *Water*, **2018**, 10(6), 738.  
268 <https://doi.org/10.3390/w10060738>
- 269 18. Vicente-Serrano, S.M.; Begueria, S.; Lopez-Moreno, J.I. A multiscalar drought index sensitive to global  
270 warming: The Standardized Precipitation Evapotranspiration Index. *J. Clim.*, **2010**, 23, 1696–1718.  
271 <https://doi.org/10.1175/2009JCLI2909.1>
- 272 19. Dee, D.P.; Uppala, S.M.; Simmons, A.J.; Berrisford, P.; Poli, P.; Kobayashi, S.; Andrae, U.; Balmaseda, M.A.;  
273 Balsamo, G.; Bauer, P.; et al. The ERA-Interim reanalysis: Configuration and performance of the data  
274 assimilation system. *Q. J. R. Meteorol. Soc.*, **2001**, 137, 553–597. <https://doi.org/10.1002/qj.828>



- 275 20. Harris, I.; Osborn, T.J.; Jones, P.; Lister, D. Version 4 of the CRU TS monthly high-resolution gridded  
276 multivariate climate dataset. *Sci. Data*, **2020**, *7*, 109. <https://doi.org/10.1038/s41597-020-0453-3>
- 277 21. Cullather, R.I.; Bromwich, D.H.; Serreze, M.C. The atmospheric hydrologic cycle over the Arctic Basin from  
278 reanalyses. Part I: Comparison with observations and previous studies, *J. Clim.*, **2000**, *13*, 923–937.  
279 [https://doi.org/10.1175/1520-0442\(2000\)013<0923:TAHCOT>2.0.CO;2](https://doi.org/10.1175/1520-0442(2000)013<0923:TAHCOT>2.0.CO;2)
- 280 22. Gimeno, L.; Stohl, A.; Trigo, R.M.; Domínguez, F.; Yoshimura, K.; Yu, L.; Drumond, A.; Durán-Quesada,  
281 A.M.; Nieto, R. Oceanic and Terrestrial Sources of Continental Precipitation. *Rev. Geophys.*, **2012**, *50*,  
282 RG4003. <https://doi.org/10.1029/2012RG000389>
- 283 23. Numaguti, A. Origin and recycling processes of precipitating water over the Eurasian continent:  
284 Experiments using an atmospheric general circulation model. *J. Geophys. Res. Atmos.*, **1999**, *104*, 1957–1972.  
285 <https://doi.org/10.1029/1998JD200026>
- 286 24. Stojanovic, M.; Drumond, A.; Nieto, R.; Gimeno, L. Variations in moisture supply from the Mediterranean  
287 Sea during meteorological drought episodes over central Europe. *Atmosphere*, **2018**, *9*, 278,  
288 <https://doi.org/10.3390/atmos9070278>
- 289 25. Vicente-Serrano, S.M.; Aguilar, E.; Martínez, R.; Martín-Hernández, N.; Azorin-Molina, C.; Sanchez-  
290 Lorenzo, A.; El Kenawy, A.; Tomás-Burguera, M.; Moran-Tejeda, E.; et al. The Complex influence of ENSO  
291 on droughts in Ecuador. *Clim. Dyn.*, **2016**, *48*, 405–427. <https://doi.org/10.1007/s00382-016-3082-y>
- 292 26. McKee, T.B.; Doesken, N.J.; Kleist, J. The relationship of drought frequency and duration to time scales. In  
293 Proceedings of the Eighth Conference on Applied Climatology, Boston, MA, USA, 17–22 January 1993; pp.  
294 179–184.  
295 [https://www.droughtmanagement.info/literature/AMS\\_Relationship\\_Drought\\_Frequency\\_Duration\\_Tim](https://www.droughtmanagement.info/literature/AMS_Relationship_Drought_Frequency_Duration_Time_Scales_1993.pdf)  
296 [e\\_Scales\\_1993.pdf](https://www.droughtmanagement.info/literature/AMS_Relationship_Drought_Frequency_Duration_Time_Scales_1993.pdf)
- 297 27. World Meteorological Organization. Drought Monitoring and Early Warning: Concepts, Progress and  
298 Future Challenges. 2006. Available online: <http://www.wamis.org/agm/pubs/brochures/WMO1006e.pdf>
- 299 28. Tan, C.; Yang, J.; Li, M. Temporal-Spatial Variation of Drought Indicated by SPI and SPEI in Ningxia Hui  
300 Autonomous Region, China. *Atmosphere*, **2015**, *6*, 1399–1421. <https://doi.org/10.3390/atmos6101399>
- 301 29. Beguería, S.; Vicente-Serrano, S.M.; Reig, F.; Latorre, B. Standardized Precipitation Evapotranspiration  
302 Index (SPEI) revisited: Parameter fitting, evapotranspiration models, tools, datasets and drought  
303 monitoring. *Int. J. Climatol.*, **2014**, *34*, 3001–3023. <https://doi.org/10.1002/joc.3887>
- 304 30. Vicente-Serrano, S.M.; Beguería, S. Short communication comment on “candidate distributions for  
305 climatological drought indices (SPI and SPEI)” by James H. Stagge et al. *Int. J. Climatol.*, **2016**, *36*, 2120–2131.  
306 <https://doi.org/10.1002/joc.4474>
- 307 31. Reboita, M.S.; Ambrizzi, T.; Silva, B.A.; Pinheiro, R.F.; Porfírio da Rocha, R. The South Atlantic Subtropical  
308 Anticyclone: Present and Future Climate. *Front. Earth Sci.*, **2019**, *7*(8), 1–15.  
309 <https://doi.org/10.3389/feart.2019.00008>
- 310 32. Nogués-Paegle, J.; Mechoso, C.R.; Fu, R.; Berbery, E.H.; Chao, W.C.; Chen, T.C.; et al. Progress in pan  
311 American CLIVAR research: understanding the south American monsoon. *Meteorologica*, **2002**, *27*, 1–30.  
312 [https://www.jsug.utexas.edu/fu/files/Nogues\\_Paegle\\_2002.pdf](https://www.jsug.utexas.edu/fu/files/Nogues_Paegle_2002.pdf)



© 2020 by the authors. Submitted for possible open access publication under the terms and conditions of the Creative Commons Attribution (CC BY) license (<http://creativecommons.org/licenses/by/4.0/>).